International Journal of Nanomedicine

Dovepress
open access to scientific and medical research

Open Access Full Text Article

ORIGINAL RESEARCH

# Formation of curcumin nanoparticles via solution-enhanced dispersion by supercritical $CO_2$

This article was published in the following Dove Press journal:
International Journal of Nanomedicine
29 April 2015
Number of times this article has been viewed

Zheng Zhao[1,3]
Maobin Xie[2]
Yi Li[2]
Aizheng Chen[4]
Gang Li[5]
Jing Zhang[2]
Huawen Hu[2]
Xinyu Wang[1,3]
Shipu Li[1,3]

[1]State Key Lab of Advanced Technology for Materials Synthesis and Processing, Wuhan University of Technology, Wuhan, People's Republic of China; [2]Institute of Textiles and Clothing, The Hong Kong Polytechnic University, Hong Kong; [3]Biomedical Materials and Engineering Research Center of Hubei Province, Wuhan University of Technology, Wuhan, People's Republic of China; [4]College of Chemical Engineering, Huaqiao University, Xiamen, People's Republic of China; [5]National Engineering Laboratory for Modern Silk, College of Textile and Clothing Engineering, Soochow University, Suzhou, People's Republic of China

**Abstract:** In order to enhance the bioavailability of poorly water-soluble curcumin, solution-enhanced dispersion by supercritical carbon dioxide ($CO_2$) (SEDS) was employed to prepare curcumin nanoparticles for the first time. A $2^4$ full factorial experiment was designed to determine optimal processing parameters and their influence on the size of the curcumin nanoparticles. Particle size was demonstrated to increase with increased temperature or flow rate of the solution, or with decreased precipitation pressure, under processing conditions with different parameters considered. The single effect of the concentration of the solution on particle size was not significant. Curcumin nanoparticles with a spherical shape and the smallest mean particle size of 325 nm were obtained when the following optimal processing conditions were adopted: P =20 MPa, T =35°C, flow rate of solution =0.5 mL·min$^{-1}$, concentration of solution =0.5%. Fourier transform infrared (FTIR) spectroscopy measurement revealed that the chemical composition of curcumin basically remained unchanged. Nevertheless, X-ray powder diffraction (XRPD) and thermal analysis indicated that the crystalline state of the original curcumin decreased after the SEDS process. The solubility and dissolution rate of the curcumin nanoparticles were found to be higher than that of the original curcumin powder (approximately 1.4 µg/mL vs 0.2 µg/mL in 180 minutes). This study revealed that supercritical $CO_2$ technologies had a great potential in fabricating nanoparticles and improving the bioavailability of poorly water-soluble drugs.

**Keywords:** curcumin, crystalline sate, dissolution rate, solubility

## Introduction

Curcumin (1,7-bis(4-hydroxy-3-methoxyphenyl)-1-6-heptadiene-3,5-dione), derived from the rhizome of the plant *Curcuma longa*, is a yellow-orange polyphenol compound. It is widely used as a spice, food preservative, and flavoring and coloring agent.[1] Curcumin exhibits many therapeutic properties, including anti-inflammation, anti-oxidation and anticancer, anti-HIV, and antimicrobial activities. Besides, it can inhibit lipid peroxidation and scavenge superoxide anion, singlet oxygen, nitric oxide, and hydroxyl radicals.[2]

Despite displaying multiple beneficial pharmacological effects, curcumin suffers from extremely low aqueous solubility in water at physiological pH.[3] The poor solubility of curcumin limits its absorption and results in low bioavailability.[4] Many new drug delivery systems have been developed to increase the aqueous solubility and the bioavailability of curcumin by using a variety of drug carriers, including liposomes,[5] phospholipid,[6] cyclodextrin,[7] chitosan nanoparticles,[8] protein nanoparticles such as silk fibroin,[9] zein,[10] and bovine serum albumin,[11] synthetic polymer nanoparticles such as PLGA,[12,13] PCL-PEG-PCL triblock copolymer,[14] and polymer nanofibers such as polyvinyl alcohol (PVA),[15] poly-(ε-caprolactone),[16] and zein.[17] Another approach for improving the bioavailability of poorly water-soluble drugs is the micronization of these drugs. Decreasing the particle size of these drugs can

Correspondence: Yi Li
Institute of Textiles and Clothing, The Hong Kong Polytechnic University, 11 Yuk Choi Road, Hung Hom, Hong Kong
Tel +852 2766 6479
Fax +852 2773 1432
Email tcliyi@polyu.edu.hk

increase their surface area, thus enhancing the solubility and dissolution rate of these drugs.[18] Recently, the wet-milling technique, a type of mechanical communication process, was used to prepare the curcumin nanoparticles of size ranging from 2 to 40 nm.[2] However, mechanical communication does not represent the ideal micronization process since both the properties of the compound and the surface properties of the particles might be altered in an uncontrolled manner. Flash nanoprecipitation from a coarse oil-in-water emulsion was developed to fabricate the curcumin nanoparticles with a mean size of about 40 nm.[19] In this process, spray-drying was employed to obtain fine curcumin powders. However, this method may suffer from the residual organic solvent and surfactants. Furthermore, spray-drying requires high temperatures and may induce denaturation of active substances.

Recently, supercritical carbon dioxide ($CO_2$) ($scCO_2$) technologies have shown great potential in the field of particle formation, especially drug micronization.[20] The $scCO_2$ technologies present many advantages, including low critical conditions ($T_c$ =304.1 K, $P_c$ =7.38 MPa), few or no solvent residue, non-flammability, low cost, and being environmentally benign.[21] So far, the most commonly used technique for particle formation using $scCO_2$ is the supercritical antisolvent (SAS) process, in which $scCO_2$ is used as an antisolvent for the precipitation of drugs dissolved in organic solvents. In the SAS process, an organic solution containing the solute is sprayed via a nozzle to a high-pressure vessel with $scCO_2$, resulting in the formation of a complete mixture of the organic solution and $scCO_2$. Continuous feeding of $scCO_2$ induces the supersaturation of active substances. Finally, particles can be precipitated in the vessel.

Solution-enhanced dispersion by $scCO_2$ (SEDS) is a modified SAS process. In this process, a solution containing the solute and $scCO_2$ are atomized via a specially designed coaxial nozzle to obtain droplets of small size and enhance mixing to increase mass transfer rates. In addition to acting as an antisolvent, $scCO_2$ is used as a "dispersing agent" to improve mass transfer between $scCO_2$ and droplets. Therefore, very small particles can be produced.[22] Particle size distribution and morphology of the solute can also be controlled by adjusting the parameters of the SEDS process, including the concentration of the solute, flow rate of the solution, temperature, and pressure of $scCO_2$. However, studies on the formation of curcumin nanoparticles by $scCO_2$ technologies, especially the SEDS process, remain unreported, although $scCO_2$ technologies offer great advantages for the formation of nanoparticles.

In the present study, the SEDS process was used to prepare curcumin nanoparticles. A full factorial experiment was designed to systematically investigate the actual effects of the processing parameters, including the flow rate of curcumin solution, precipitation pressure, concentration of curcumin solution, and precipitation temperature, on particle size. Fourier transform infrared (FTIR) spectroscopy measurement, X-ray powder diffraction (XRPD), differential scanning calorimetry (DSC), and thermogravimetric (TG) analysis were used to study the chemical and physical properties of the nanoparticles fabricated using the SEDS process. Furthermore, the solubility and dissolution rate of curcumin were also measured to evaluate its pharmaceutical performance.

## Materials and methods

### Materials

Curcumin was purchased from International Laboratory (USA). $CO_2$ with a purity of 99.9% was supplied by Hong Kong Specialty Gases Co., Ltd. (Hong Kong). The solvent, acetone, was purchased from Advanced Technology & Industrial Co., Ltd. (Hong Kong). All other compounds were of analytical purity.

### Preparation of curcumin nanoparticles by the SEDS process

The experimental apparatus of the SEDS process consists of three major sections: a $CO_2$ supply system, an organic solution delivery system, and a high-pressure vessel. The schematic diagram of the SEDS process is shown in Figure 1. In this process, when the desired experimental conditions were reached, curcumin dissolved in acetone was injected into the high-pressure vessel via a stainless steel coaxial nozzle simultaneously with $scCO_2$ using a high performance liquid chromatography pump. After all the solution was delivered into the high-pressure vessel, fresh $CO_2$ was pumped to wash precipitated particles for about 30 minutes to eliminate any residual organic solvent. During the washing process, the precipitation temperature and pressure were maintained as described above. After the washing process, the $CO_2$ flow was stopped and the $CO_2$ in the high-pressure vessel was slowly depressurized to atmospheric pressure. The curcumin nanoparticles were then collected on the filter at the bottom of the high-pressure vessel for characterization.

### Full factorial designs (FFD)

To investigate the influence and significance of the four process parameters (the flow rate of curcumin solution, precipitation pressure, concentration of curcumin solution and precipitation temperature) in the SEDS process on both the morphology and particle size of curcumin nanoparticles,

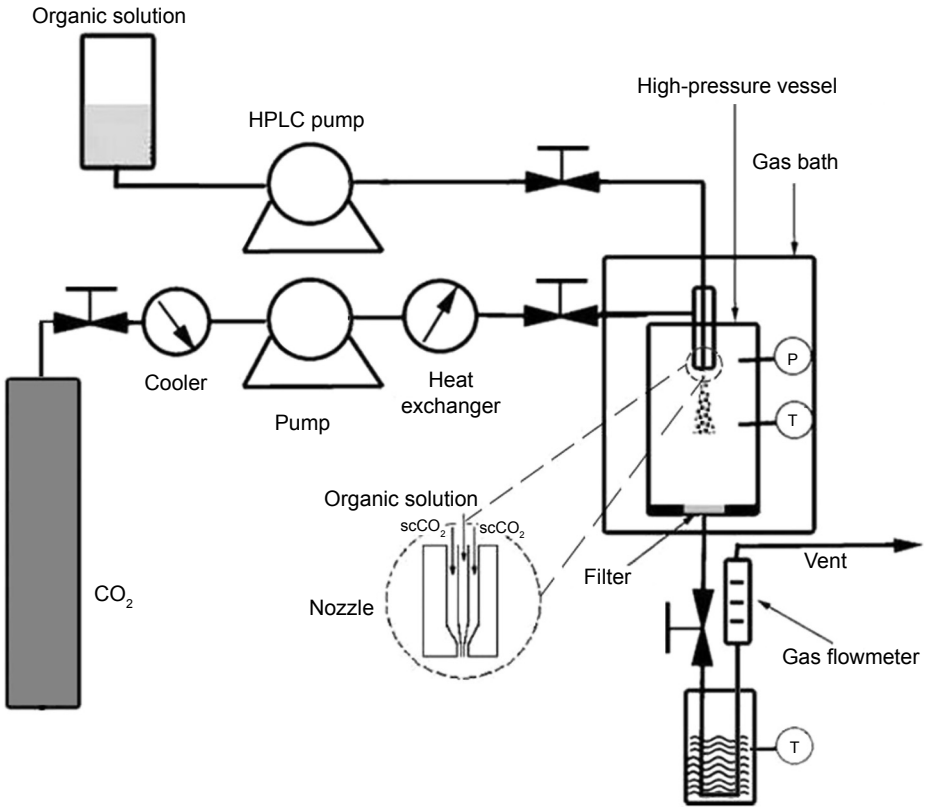


**Figure 1** Schematic diagram of the SEDS process.
**Abbreviation:** SEDS, solution-enhanced dispersion by supercritical carbon dioxide ($CO_2$); P, pressure; T, temperature; HPLC, high performance liquid chromatography.

a $2^4$ full factorial experiment, was designed and conducted, as shown in Table 1. According to FFD, there are 16 experiments (shown in Table 2). The MINITAB software version 15 was applied to set the experiments and analyze the experimental data.

## Surface morphology, particle size, and particle size distribution

The surface morphology of curcumin nanoparticles was visualized by scanning electron microscopy (FE-SEM) (JSM-6490; JEOL, Tokyo, Japan). Before analysis, samples were attached onto carbon paint and placed on an aluminum sample holder. These samples were then gold sputter-coated under argon prior to imaging. Curcumin nanoparticles were made conductive by sputtering a thin layer of gold onto their surface. The particle size and particle size distribution of the samples were analyzed by SmileView software from the SEM photographs.

**Table 1** Experimental factors and levels

| Symbols | Factors | Coded level | |
|---|---|---|---|
| | | −1 | +1 |
| A | Pressure (MPa) | 10 | 20 |
| B | Temperature (°C) | 35 | 45 |
| C | Flow rate of solution (mL·min$^{-1}$) | 0.5 | 1 |
| D | Concentration (%) | 0.5 | 1 |

**Notes:** Precipitation pressure (**A**), precipitation temperature (**B**), flow rate of curcumin solution (**C**), concentration of curcumin solution (**D**).

**Table 2** Experimental design and results of full factorial design

| Run order | A | B | C | D | Mean size (nm) | SD |
|---|---|---|---|---|---|---|
| 1 | 1 | −1 | −1 | −1 | 389 | 61 |
| 2 | 1 | −1 | −1 | −1 | 325 | 21 |
| 3 | −1 | 1 | −1 | −1 | 694 | 64 |
| 4 | 1 | 1 | −1 | −1 | 337 | 12 |
| 5 | −1 | −1 | 1 | −1 | 547 | 44 |
| 6 | 1 | −1 | 1 | −1 | 386 | 16 |
| 7 | −1 | 1 | 1 | −1 | 1,024 | 58 |
| 8 | 1 | 1 | 1 | −1 | 370 | 4 |
| 9 | −1 | −1 | −1 | 1 | 427 | 53 |
| 10 | 1 | −1 | −1 | 1 | 368 | 24 |
| 11 | −1 | 1 | −1 | 1 | 483 | 9 |
| 12 | 1 | 1 | −1 | 1 | 372 | 53 |
| 13 | −1 | −1 | 1 | 1 | 374 | 19 |
| 14 | 1 | −1 | 1 | 1 | 334 | 30 |
| 15 | −1 | 1 | 1 | 1 | 899 | 163 |
| 16 | 1 | 1 | 1 | 1 | 692 | 118 |

**Notes:** Precipitation pressure (**A**), precipitation temperature (**B**), flow rate of curcumin solution (**C**), concentration of curcumin solution (**D**).

## FTIR analysis

The samples were combined with potassium bromide, and the mixtures of the samples and potassium bromide were pressed into a transparent tablet. The FTIR spectra for the samples were recorded on an FTIR Perkin Elmer 1720 (Perkin Elmer, USA) in the transmission mode with the wave number ranging from 4,000 to 400 $cm^{-1}$.

## XRPD analysis

XRPD was performed by an X-ray diffractometer with a Cu Kα (λ =1.5405 Å) radiation (D8 Advance; Bruker AXS, Germany). The measurement was carried out in a 2θ range of 5°~45° with a 0.02° step size and 10° $min^{-1}$ scan speed with a 2 D detector at 40 kV and 40 mA.

## Thermal analysis

DSC samples were analyzed by DSC thermogram analysis (Simultaneous Thermal Analyzer [STA] 6000; Perkin Elmer, MA, USA) at a heating rate of 10°C $min^{-1}$ over a temperature range of 25°C–400°C in a nitrogen ($N_2$) atmosphere. Each sample was sealed separately in a standard aluminum pan. TG analysis was carried out using a Shimadzu TG analyzer (TGA50; Kyoto, Japan) in a nitrogen atmosphere. The heating rate of the experiment was 10°C $min^{-1}$. Nitrogen flow was maintained at 50 mL·$min^{-1}$.

## Solubility and dissolution rate measurements

Solubility and dissolution rate tests of the original curcumin and the curcumin nanoparticles were conducted using a modified dialysis bag method. An excessive amount of each sample (10 mg) was dispersed in 5 mL of PBS (pH 7.4) and placed in a pretreated dialysis bag (Molecular Weight: 12,000–14,000 Daltons), and then the bag was put into 50 mL of PBS and incubated in a water bath at 37°C and 60 rpm. At a specific time, 1 mL of the solution was removed, followed by centrifugation (10,000× *g*, 10 minutes). Next, the concentration of the supernatant was detected by UV spectrometry (PerkinElmer Lambda 18; USA) at 410 nm. The dissolution rate was calculated in terms of the curcumin concentration and incubation time. Each experiment was carried out in triplicate.

# Results and discussion

## Surface morphology and particle size of curcumin nanoparticles

Figure 2 shows the surface morphology of the original curcumin powders before the SEDS process. The original curcumin powders were irregular and exhibited a mean size of approximately 3.58 μm. The experimental design and results of $2^4$ FFD experiments are presented in Table 2. Figure 3 shows the SEM micrographs of the curcumin nanoparticles fabricated by the SEDS process in different runs, the details of which are listed in Table 2. It can be concluded from Figure 3 that the curcumin nanoparticles possessed an irregular spherical morphology with a mean particle size from approximately 325 to 1,024 nm. The surface morphology of the biggest and smallest curcumin particles are shown in Figure 3A and B, respectively. Therefore, optimal conditions for preparing the smallest curcumin nanoparticles (325 nm) were as follows: P =20 MPa; T =35°C; flow rate of the solution =0.5 mL·$min^{-1}$; and concentration of the solution =0.5%. Evidently, the SEDS process is an effective way to prepare curcumin nanoparticles. Moreover, by adjusting the different process parameters of the SEDS process, curcumin nanoparticles with controllable particle size can be prepared successfully.

## Influence of process parameters on particle size

The FFD is a suitable technique to estimate the effects of process parameters on the process outcomes. For the evaluation of the main effect of process parameters including the precipitation pressure (A), precipitation temperature (B), flow rate of curcumin solution (C), and concentration of curcumin solution (D) on the mean particle size of curcumin nanoparticles, the quantitative data analysis for the results shown in Table 2 was performed. Figures 4 and 5 shows the standardized effect of the factors on particle size and the main effects plot for particle size, respectively. Table 3 lists the estimated effects and coefficients for particle size.

As shown in Figure 4 and Table 3, A–C ($P<0.05$) significantly affected the size of curcumin nanoparticles. However, D ($P>0.05$) had an insignificant effect on particle size.

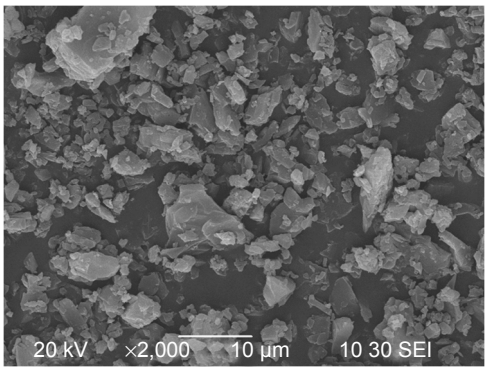


**Figure 2** SEM micrograph of the original curcumin powders.
**Abbreviation:** SEM, scanning electron microscopy.

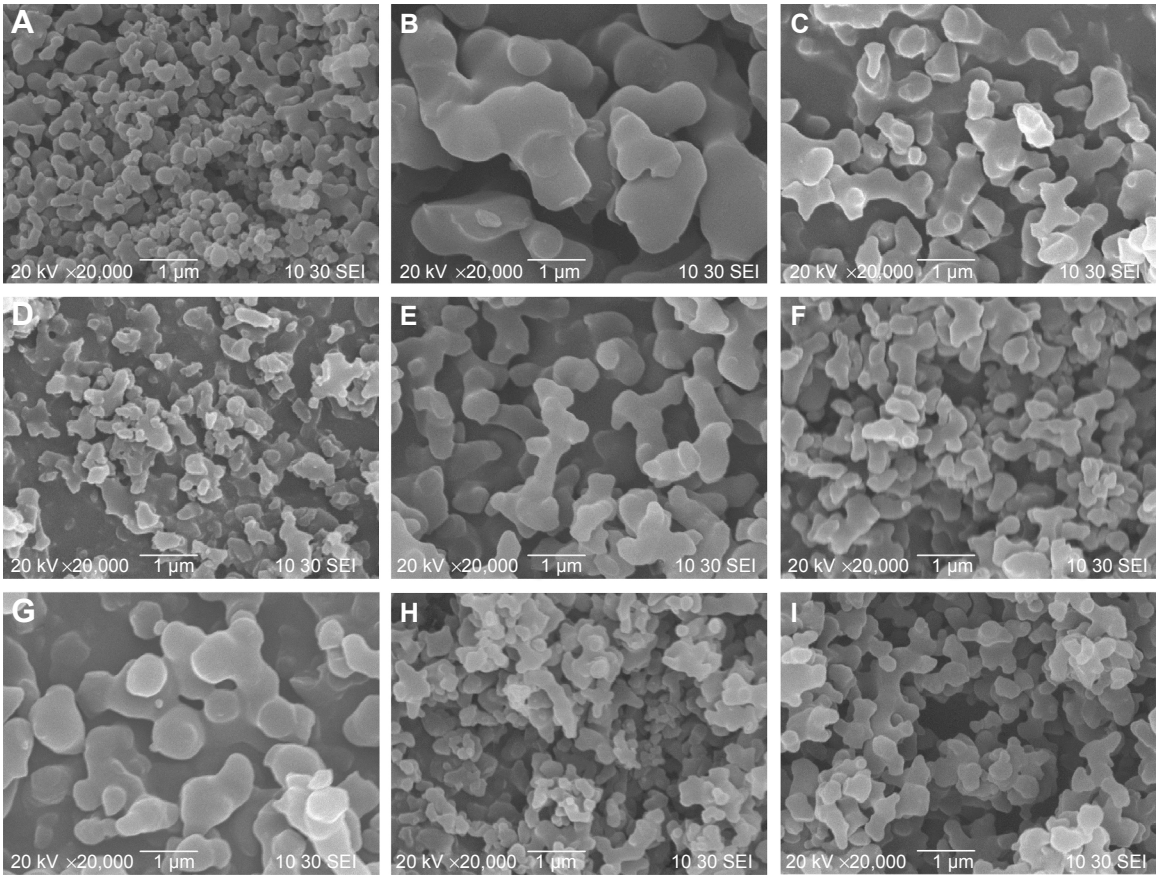


**Figure 3** SEM micrographs of curcumin nanoparticles prepared by the SEDS process under different conditions (**A**) 0.5%-35°C-0.5 mL/min-20 Mpa; (**B**) 0.5%-45°C-1 mL/min-10 Mpa; (**C**) 0.5%-45°C-0.5 mL/min-10 Mpa; (**D**) 5%-45°C-0.5 mL/min-20 Mpa; (**E**) 0.5%-35°C-1 mL/min-10 Mpa; (**F**) 1%-45°C-0.5 mL/min-20 Mpa; (**G**) 1%-45°C-1 mL/min-20 Mpa; (**H**) 1%-35°C-1 mL/min-20 Mpa; (**I**) 0.5%-35°C-1 mL/min-20 Mpa.
**Abbreviations:** SEM, scanning electron microscopy; SEDS, solution-enhanced dispersion by supercritical carbon dioxide ($CO_2$).

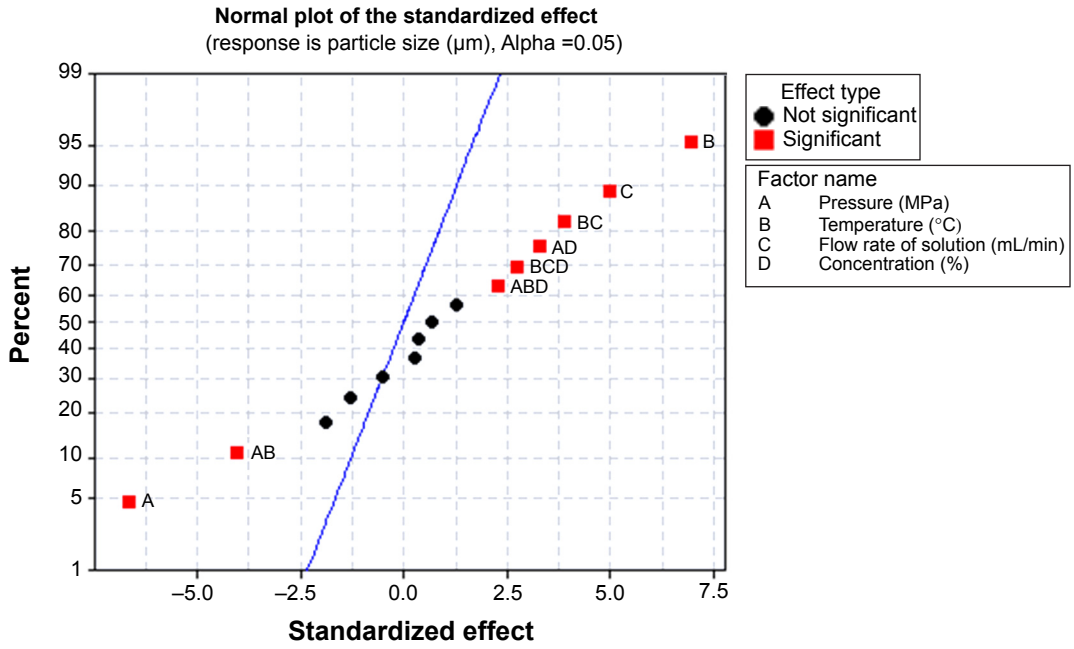


**Figure 4** Standardized effect of the factors on particle size.

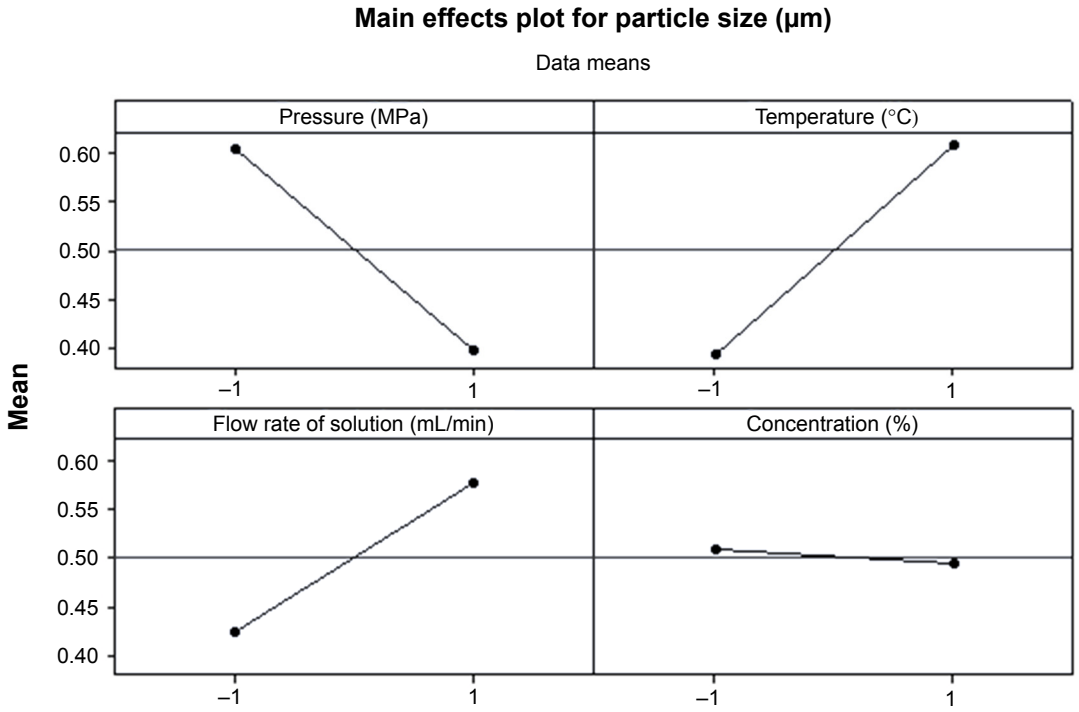


**Figure 5** Main effects plot for particle size.

According to the slopes of the lines in Figure 5, the order of importance of the factors affecting particle size can be summarized as follows: B > A > D > C. Within the range of parameters studied, particle size increased with increased temperature or flow rate of solution, and decreased precipitation pressure. The effect of concentration of the solution alone on particle size was not significant, and decreasing the concentration can reduce the particle size of curcumin nanoparticles slightly.

## Effect of precipitation pressure

As shown in Figure 5, an increase in the precipitation pressure induced a reduction in the particle size of curcumin. Runs 3 and 4 (Table 2) show that increasing the pressure from 10 to 20 Mpa led to a decrease in the particle size of curcumin nanoparticles from 694 to 337 nm. This trend was also observed in the morphology of curcumin nanoparticles shown in Figure 3C and D. Zhao et al also reported a similar phenomenon.[23]

**Table 3** Estimated effects and coefficients for particle size (nm) (coded units)

| Term | Effect | Coef | SE coef | T | P |
|---|---|---|---|---|---|
| Constant | | 0.5011 | 0.01552 | 32.29 | 0.000 |
| Pressure (MPa) | –0.2064 | –0.1032 | 0.01552 | –6.65 | 0.000 |
| Temperature (°C) | 0.2152 | 0.1076 | 0.01552 | 6.93 | 0.000 |
| Flow rate of solution (mL/min) | 0.1539 | 0.0770 | 0.01552 | 4.96 | 0.000 |
| Concentration (%) | –0.0152 | –0.0076 | 0.01552 | –0.49 | 0.631 |

**Abbreviations:** T, temperature; P, pressure; Coef, coefficient; SE coef, standard error coefficient.

The nucleation and growth mechanism induced by supersaturation can be used to explain the result. In the SEDS process, mutual diffusion between the liquid solution and $scCO_2$ resulted in phase separation and supersaturation of the solution, thus leading to the nucleation and precipitation of particles. Lower supersaturation ratios resulted in fewer nuclei, which in turn yielded larger particles. An increase in pressure led to an increase in the $CO_2$ density and mole fraction, thereby enhancing the antisolvent effect of $scCO_2$. Therefore, supersaturation within the liquid phase was more quickly reached, preventing the crystals from growing and inducing the formation of particles of smaller size.[24]

## Effect of precipitation temperature

Figures 4 and 5 show that precipitation temperature significantly influenced particle size, and increasing the temperature causes an increase in the particle size of curcumin nanoparticles. Runs 5 and 7 (Table 2) indicated that an increase in temperature from 35°C to 45°C would result in an increase in the size of curcumin nanoparticles from 547 to 1,024 nm. These

results were supported by surface morphologies shown in Figure 3B and E.

Temperature can affect the density of supercritical fluid. A small change in the precipitation temperature can lead to considerable density changes, especially near the critical point.[25] The increased in temperature caused decreased density of $scCO_2$, thus resulting in a decrease of the antisolvent effect of $scCO_2$. Therefore, achieving supersaturation was slowed and a bigger particle was formed. Similar results were also observed in other studies.[26]

## Effect of flow rate of solution

Figures 4 and 5 show that the flow rate of the solution significantly affected the size of curcumin nanoparticle, and a higher flow rate of the solution resulted in smaller particles. When the flow rate of curcumin solution was raised from 0.5 to 1 $mL \cdot min^{-1}$ as indicated in Figure 3F and G, the size of curcumin nanoparticles increased from 372 nm of Run 12 to 692 nm of Run 16 (Table 2).

An increased in the flow rate of the solution resulted in increased solution content in the precipitator within the same time and decreased the antisolvent effect of $scCO_2$, thus reducing the achievable supersaturation ratio. Lower supersaturation ratios generated fewer nuclei, which in turn yielded larger particles. Additionally, the micronization process shifted toward the growth process, and so, larger particles were produced.[27] Previous researchers have also reported similar results.[28,29]

## Effect of concentration of solution

As indicated in Figures 4 and 5, the concentration of solution had a slight effect on particle size; hence, the higher the concentration of solution, the smaller the particle size. Runs 6 and 14 (Table 2) showed that an increase in the concentration of curcumin solution from 0.5% to 1% can decrease the size of curcumin nanoparticles from 386 to 334 nm. Surface morphologies shown in Figure 3H and I demonstrated this trend. Chen et al reported similar results.[30]

This finding can be explained by considering that a higher condensation rate from a higher concentration tended to result in a higher supersaturation, and thus smaller particles were expected.[31] It is consistent with the classical nucleation and growth theory. However, in the operating conditions, the concentration of solution affected the particle size of curcumin nanoparticles slightly.

## FTIR analysis

FTIR can reveal the chemical changes by producing an infrared absorption spectrum. Figure 6 shows the FTIR spectra of original curcumin and curcumin nanoparticles prepared by the SEDS process under optimal conditions. It can be seen that FTIR spectra of original curcumin and curcumin nanoparticles prepared by the SEDS process did not show significant differences. Thus, there is no change in the chemical composition of the samples before and after the SEDS process. The characteristic peaks at 1,581 $cm^{-1}$, 1,511 $cm^{-1}$, 1,279 $cm^{-1}$, and 1,152 $cm^{-1}$ were attributed to the stretching

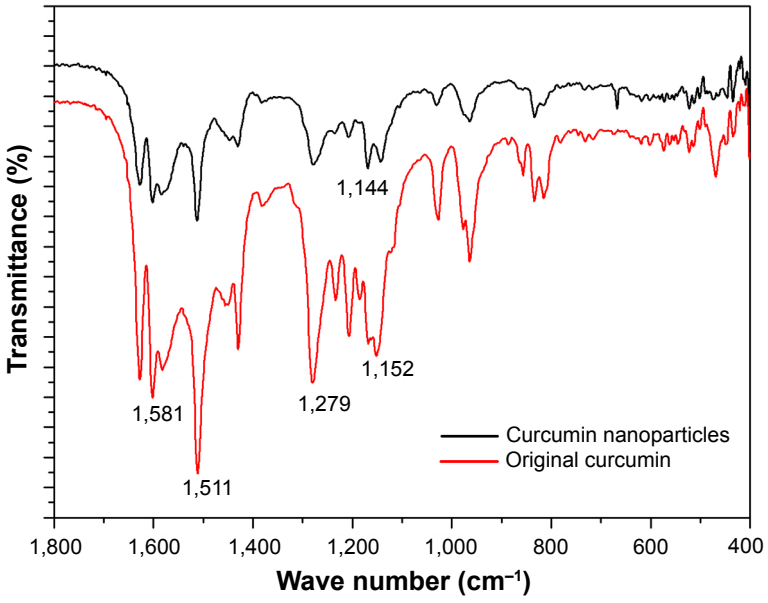


**Figure 6** FTIR spectra of original curcumin and curcumin nanoparticles prepared by the SEDS process under optimal conditions.
**Abbreviations:** FTIR, Fourier transform infrared; SEDS, solution-enhanced dispersion by supercritical carbon dioxide ($CO_2$).

vibrations of the benzene ring, C=C vibrations, aromatic C-O stretching, and C-O-C stretching modes, respectively, in original curcumin.[14] After the SEDS process, the main peak at 1,152 $cm^{-1}$ found in the FTIR spectra of original curcumin shifted to 1,144 $cm^{-1}$. This finding indicated that minor structural changes occurred at the molecular level. A previous study also reported such a minor structure change of samples after the supercritical $CO_2$ process.[30] However, no observable new characteristic peaks were found in the FTIR spectra of curcumin nanoparticles. Therefore, there was no change in the chemical composition of the samples before and after the SEDS process.

## XRPD analysis

XRPD is an important technique employed to determine the crystal phase of the samples. Figure 7 shows the XRPD pattern of original curcumin and curcumin nanoparticles prepared by the SEDS process under optimal conditions. The characteristic high-intensity diffraction peaks of the original curcumin indicated it was in a highly crystalline form before the SEDS process.[32] However, the intensity of these characteristic diffraction peaks weakened after the SEDS process. Curcumin nanoparticles showed a lower value for the peak areas (indicative of crystallinity) than that of original curcumin (556.5 vs 828.3). Furthermore, the peaks at $2\theta=13.4°$, 16.3°, 20.1°, and 21.8° disappeared. These results demonstrated that the precipitation by the SEDS process decreased the crystallinity of the original curcumin, and the curcumin nanoparticles exhibited a more amorphous state than original curcumin. A crystalline-amorphous transition resulted in excess free energy and entropy. Compared with the crystalline state, the amorphous state was thermodynamically less stable.[31] Consequently, the decreased crystallinity of original curcumin by the SEDS process favors an increased dissolution rate of a drug powder.

## Thermal analysis

DSC is widely used to characterize the thermal behavior of various materials, such as melting and crystallization behaviors. The DSC curves of original curcumin and curcumin nanoparticles prepared by the SEDS process under optimal conditions are given in Figure 8. For original curcumin, a sharp peak at 164.4°C corresponding with the melting point was found.[33] After the SEDS process, the melting point of curcumin was unchanged and a sharp peak at 164.4°C was still observed for curcumin nanoparticles. However, curcumin nanoparticles showed a lower value for the endothermic peak areas (indicative of the crystallization extent) than that of original curcumin (705.4 $J \cdot g^{-1}$ vs 985.1 $J \cdot g^{-1}$). The reduction in the integral area can be attributed to the

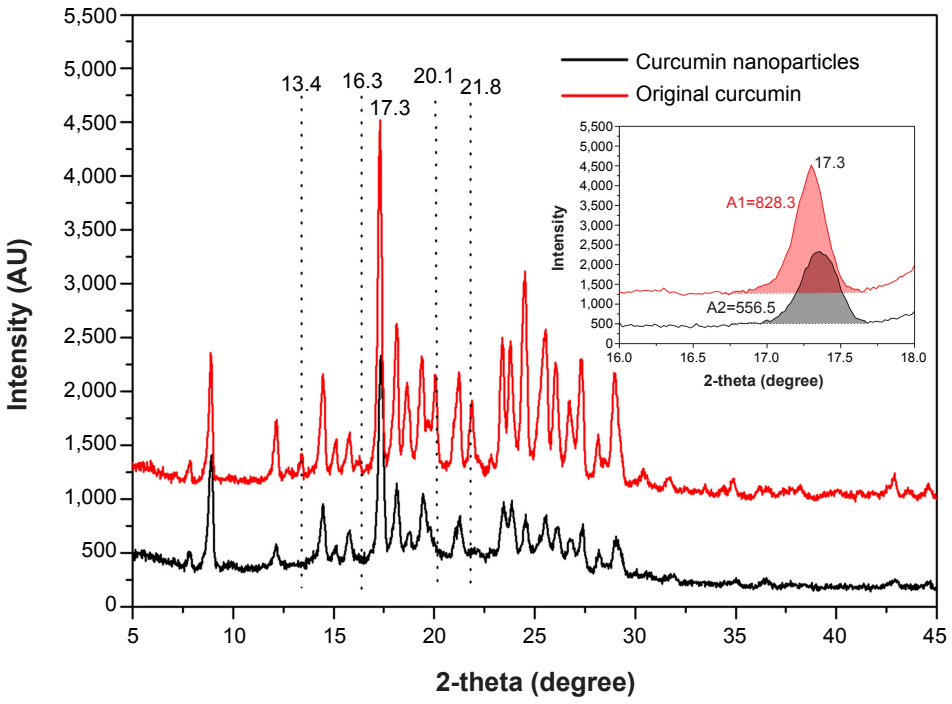


**Figure 7** XRPD pattern of original curcumin and curcumin nanoparticles prepared by the SEDS process under optimal conditions. Figure 7 inset is a partially enlarged view.
**Abbreviations:** XRPD, X-ray powder diffraction; SEDS, solution-enhanced dispersion by supercritical carbon dioxide ($CO_2$).

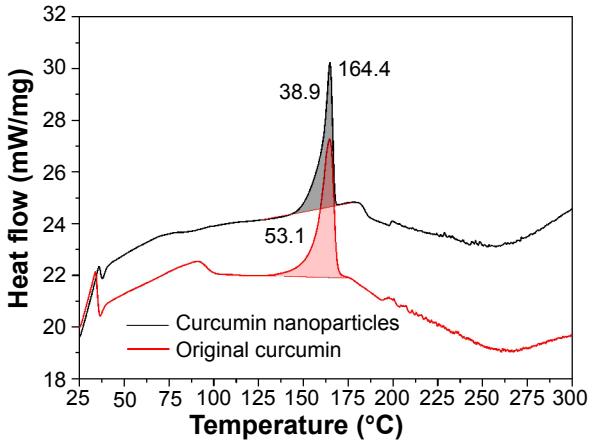


**Figure 8** DSC curves of original curcumin and curcumin nanoparticles prepared by the SEDS process under optimal conditions.
**Abbreviations:** DSC, differential scanning calorimetry; SEDS, solution-enhanced dispersion by supercritical carbon dioxide ($CO_2$).

disrupted molecule chains and the decreased crystallization extent caused by the SEDS process. This result was consistent with that of XRPD analysis.

TG curves corresponding with the thermal weight losses of original curcumin and the curcumin nanoparticles prepared by the SEDS process under optimal conditions are shown in Figure 9. Upon heating, original curcumin suffered a pronounced weight loss step occurring near 100°C that can be ascribed to the loss of water composition. However, weight loss was not observed in the curcumin nanoparticles. In addition, based on the tangent method, the decomposition temperatures of original curcumin and curcumin nanoparticles were found to be 273.6°C and 266.7°C, respectively. Thus, the thermal stability of curcumin decreased after the SEDS process owing to decreased crystalline structure. The result well agreed with those of DSC and XPRD analyses.

## Solubility and dissolution rate

Figure 10 shows the dissolution profiles of original curcumin and curcumin nanoparticles prepared by the SEDS process under optimal conditions. The kinetic solubility curve of original curcumin very quickly reached the plateau. The maximum solubility of original curcumin was about 0.2 µg/mL at 60 minutes. After the SEDS process, the resulting curcumin nanoparticles exhibited a maximum solubility of approximately 1.4 µg/mL. Moreover, the dissolution rate of curcumin nanoparticles was higher than that of original curcumin, particularly in the first 180 minutes. The dramatically increased dissolution rate and solubility of curcumin nanoparticles can be attributed to the increased specific surface area for better wettability resulting from the reduced particle size. Curcumin nanoparticles also exhibited less crystallinity than original curcumin. A decrease in crystallinity resulted in decreased thermodynamic stability, thereby favoring increased dissolution rate and bioavailability of curcumin powder.

# Conclusion

Curcumin nanoparticles were fabricated for the first time using SEDS. The investigation using $2^4$ FFD indicated that an increase in the flow rate of curcumin solution and the precipitation temperature increased the size of curcumin nanoparticles, whereas a reduction in the precipitation pressure increased the particle size. The single effect of the concentration of the solution on particle size was insignificant.

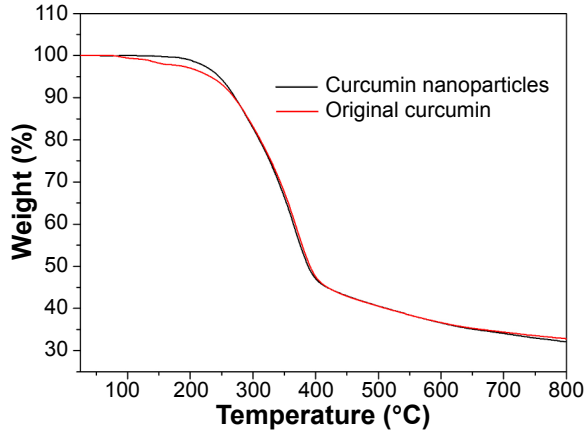


**Figure 9** TG curves of original curcumin and curcumin nanoparticles prepared by the SEDS process under optimal conditions.
**Abbreviations:** TG, thermogravimetric; SEDS, solution-enhanced dispersion by supercritical carbon dioxide ($CO_2$).

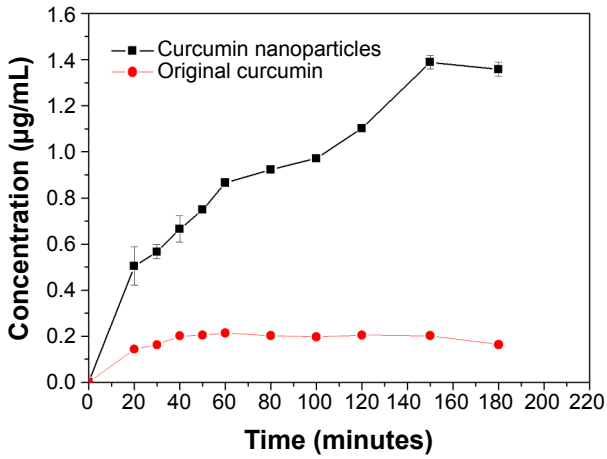


**Figure 10** Dissolution profiles of original curcumin and curcumin nanoparticles prepared by the SEDS process under optimal conditions.
**Abbreviation:** SEDS, solution-enhanced dispersion by supercritical carbon dioxide ($CO_2$).

Given the reduction in particle size and crystallinity, the fabricated curcumin nanoparticles possessed higher solubility and hence a higher dissolution rate than original curcumin. These results demonstrated that the SEDS process is an effective method for preparing curcumin nanoparticles and improving the solubility and dissolution rate of poorly water-soluble drugs.

## Acknowledgments

We thank the Hong Kong Research Grant Council and the Hong Kong Polytechnic University through projects PolyU5242/09E and G-YM63. We would also like to thank the support provided by the Natural Science Foundation of Hubei Province through project 2014CFB839, Doctoral Research Fund of Wuhan University of Technology through project 471-40120093, Guangdong Provincial Department of Science and Technology through projects 2012B050800002 and 2012B091000143.

## Disclosure

The authors report no conflicts of interest in this work.

## References

1. Sun Y, Du L, Liu Y, et al. Transdermal delivery of the in situ hydrogels of curcumin and its inclusion complexes of hydroxypropyl-β-cyclodextrin for melanoma treatment. *Int J Pharm*. 2014;469(1):31–39.
2. Bhawana, Basniwal RK, Buttar HS, Jain VK, Jain N. Curcumin nanoparticles: preparation, characterization, and antimicrobial study. *J Agr Food Chem*. 2011;59(5):2056–2061.
3. Yallapu MM, Jaggi M, Chauhan SC. Curcumin nanoformulations: a future nanomedicine for cancer. *Drug Discov Today*. 2012; 17(1–2):71–80.
4. Anand P, Kunnumakkara AB, Newman RA, Aggarwal BB. Bioavailability of curcumin: problems and promises. *Mol Pharm*. 2007; 4(6):807–818.
5. Takahashi M, Uechi S, Takara K, Asikin Y, Wada K. Evaluation of an oral carrier system in rats: bioavailability and antioxidant properties of liposome-encapsulated curcumin. *J Agr Food Chem*. 2009; 57(19):9141–9146.
6. Maiti K, Mukherjee K, Gantait A, Saha BP, Mukherjee PK. Curcumin-phospholipid complex: preparation, therapeutic evaluation and pharmacokinetic study in rats. *Int J Pharm*. 2007;330(1–2):155–163.
7. Marcolino VA, Zanin GM, Durrant LR, Benassi MDT, Matioli G. Interaction of curcumin and bixin with β-cyclodextrin: complexation methods, stability, and applications in food. *J Agr Food Chem*. 2011; 59(7):3348–3357.
8. Akhtar F, Rizvi MM, Kar SK. Oral delivery of curcumin bound to chitosan nanoparticles cured *Plasmodium yoelii* infected mice. *Biotechnol Adv*. 2012;30(1):310–320.
9. Gupta V, Aseh A, Rios CN, Aggarwal BB, Mathur AB. Fabrication and characterization of silk fibroin-derived curcumin nanoparticles for cancer therapy. *Int J Nanomed*. 2009;4(1):115–122.
10. Patel A, Hu YC, Tiwari JK. Synthesis and characterization of zein-curcumin colloidal particles. *Soft Matter*. 2010;6(24):6192–6199.
11. Jithan AV, Madhavi K, Madhavi M, Prabhakar K. Preparation and characterization of albumin nanoparticles encapsulating curcumin intended for the treatment of breast cancer. *Int J Pharm Invest*. 2011; 1(2):119–125.
12. Beloqui A, Coco R, Memvanga PB, Ucakar B, des Rieux A, Préat V. pH-sensitive nanoparticles for colonic delivery of curcumin in inflammatory bowel disease. *Int J Pharm*. 2014;473(1–2):203–212.
13. Yallapu MM, Gupta BK, Jaggi M, Chauhan SC. Fabrication of curcumin encapsulated PLGA nanoparticles for improved therapeutic effects in metastatic cancer cells. *J Colloid Interf Sci*. 2010;35(1):19–29.
14. Feng R, Song Z, Zhai G. Preparation and in vivo pharmacokinetics of curcumin-loaded PCL-PEG-PCL triblock copolymeric nanoparticles. *Int J Nanomedicine*. 2012;7:4089–4098.
15. Sun XZ, Williams GR, Hou XX, Zhu LM. Electrospun curcumin-loaded fibers with potential biomedical applications. *Carbohyd Polym*. 2013;94(1):147–153.
16. Merrell JG, McLaughlinb SW, Tie L, Laurencind CT, Chen AF, Nair LS. Curcumin loaded poly(ε-caprolactone) nanofibers: wound dressing with antioxidant and anti-inflammatory properties. *Clin Exp Pharmacol P*. 2009;36(12):1149–1156.
17. Brahatheeswaran D, Mathew A, Aswathy RG, et al. Hybrid fluorescent curcumin loaded zein electrospun nanofibrous scaffold for biomedical applications. *Biomed Mater*. 2012;7(4):045001.
18. Tagami T, Imao Y, Ito S, Nakada A, Ozeki T. Simple and effective preparation of nano-pulverized curcumin by femtosecond laser ablation and the cytotoxic effect on C6 rat glioma cells *in vitro*. *Int J Pharm*. 2014;468(1–2):91–96.
19. Margulis K, Magdassi S, Lee HS, Macosko CW. Formation of curcumin nanoparticles by flash nanoprecipitation from emulsions. *J Colloid Interface Sci*. 2014;434:65–70.
20. Liu G, Wang W, Wang H, Jiang Y. Preparation of 10-hydroxycamptothecin proliposomes by the supercritical $CO_2$ anti-solvent process. *Chem Eng J*. 2014;243:289–296.
21. Zhao Z, Chen AZ, Li Y, et al. Fabrication of silk fibroin nanoparticles for controlled drug delivery. *J Nanopart Res*. 2012;14(4):736–745.
22. Zhao Z, Li Y, Zhang Y, et al. Development of silk fibroin modified poly(l-lactide)-poly(ethylene glycol)-poly(l-lactide) nanoparticles in supercritical $CO_2$. *Powder Technol*. 2014;268:118–125.
23. Zhao Z, Li Y, Chen AZ, et al. Generation of silk fibroin nanoparticles via solution-enhanced dispersion by supercritical $CO_2$. *Ind Eng Chem Res*. 2013;52(10):3752–3761.
24. Jin HY, Hemingway M, Xia F, Li NS, Zhao YP. Production of β-Carotene nanoparticles by the solution enhanced dispersion with enhanced mass transfer by ultrasound in supercritical $CO_2$ (SEDS-EM). *Ind Eng Chem Res*. 2011;50(23):13475–13484.
25. Kalani M, Yunus R. Application of supercritical antisolvent method in drug encapsulation: a review. *Int J Nanomedicine*. 2011;6: 1429–1442.
26. Lee BM, Kim SJ, Lee BC, Kim HS, Kim H, Lee YW. Preparation of micronized β-HMX using supercritical carbon dioxide as antisolvent. *Ind Eng Chem Res*. 2011;50(15):9107–9115.
27. Wang Q, Guan YX, Yao SJ, Zhu ZQ. Microparticle formation of sodium cellulose sulfate using supercritical fluid assisted atomization introduced by hydrodynamic cavitation mixer. *Chem Eng J*. 2010;159:220–229.
28. Reverchon E, De Marco I. Supercritical antisolvent precipitation of cephalosporins. *Powder Technol*. 2006;164(3):139–146.
29. Su CS, Lo WS, Lien LH. Micronization of fluticasone propionate using supercritical antisolvent process. *Chem Eng Technol*. 2011;34(4): 535–541.
30. Chen AZ, Li L, Wang SB, et al. Nanonization of methotrexate by solution-enhanced dispersion by supercritical $CO_2$. *J Supercrit Fluid*. 2012;67:7–13.
31. Montes A, Tenorio A, Gordill MD, Pereyra C, Martinez de la Ossa EJ. Screening design of experiment applied to supercritical antisolvent precipitation of amoxicillin: exploring new miscible conditions. *J Supercrit Fluid*. 2010;51:399–403.
32. Song Z, Zhu W, Liu N, Yang F, Feng R. Linolenic acid-modified PEG-PCL micelles for curcumin delivery. *Int J Pharm*. 2014;471(1–2):312–321.
33. Xie X, Tao Q, Zou Y, et al. PLGA nanoparticles improve the oral bioavailability of curcumin in rats: characterizations and mechanisms. *J Agr Food Chem*. 2011;59(17):9280–9289.